Low-noise Brillouin laser on a chip at 1064 nm

Jiang Li, Hansuek Lee, and Kerry J. Vahala*

T. J. Watson Laboratory of Applied Physics, California Institute of Technology, Pasadena, California 91125, USA
**Corresponding author: vahala@caltech.edu*

Received October 25, 2013; accepted November 15, 2013;
posted December 3, 2013 (Doc. ID 200164); published January 8, 2014

We demonstrate narrow-linewidth-stimulated Brillouin lasers at 1064 nm from ultra-high-Q silica wedge disk resonators on silicon. Fundamental Schawlow–Townes frequency noise of the laser is on the order of 0.1 Hz^2/Hz. The technical noise spectrum of the on-chip Brillouin laser is close to the thermodynamic noise limit of the resonator (thermorefractive noise) and is comparable to that of ultra-narrow-linewidth Nd:YAG lasers. The relative intensity noise of the Brillouin laser also is reduced by using an intensity-stabilized pump laser. Finally, low-noise microwave synthesis up to 32 GHz is demonstrated by heterodyne of first and third Brillouin Stokes lines from a single resonator.

OCIS codes: (190.5890) Scattering, stimulated; (290.5900) Scattering, stimulated Brillouin; (190.4390) Nonlinear optics, integrated optics.
http://dx.doi.org/10.1364/OL.39.000287

Low phase (frequency) noise lasers are critical in a variety of scientific, commercial, and military applications, including spectroscopy [1], optical clocks [2], coherent fiber-optic communication [3], microwave photonics [4], and remote sensing [5]. Among various laser technologies to achieve low phase noise, stimulated Brillouin scattering involves the nonlinear interaction among the pump, Stokes, and acoustic fields. Due to stronger damping of the acoustic field relative to the optical fields, the frequency noise of the Brillouin laser is greatly suppressed relative to the pump laser frequency noise [6,7]. Brillouin fiber ring lasers with narrow linewidth on the order of 10 Hz to 1 kHz have been demonstrated [8,9]. Also Brillouin lasers have been demonstrated from ultra-high-Q bulk microcavities [7,10] and chip-based Chalcogenide waveguides [11]. Moreover, precise matching of the free-spectral range (FSR) to the Brillouin shift (necessary for efficient laser operation) has been recently demonstrated using a silica ultra-high-Q resonator on silicon [12]. For operation in the 1550 nm band, these devices also have record-low fundamental frequency noise (Schawlow–Townes noise) for a chip-based laser [12,13] and furthermore have been used to demonstrate microwave synthesis up to 22 GHz using cascaded oscillation in a single resonator [14].

In this Letter, we study the operation of these devices at 1064 nm by pumping using a narrow-linewidth Ytterbium-doped fiber laser. In addition to characterization of the laser frequency noise, we investigate the laser relative intensity noise (RIN) of these devices for the first time. Overall, the fundamental and technical frequency noise of the laser is greatly suppressed relative to the pump laser and is comparable with that of low-noise Nd:YAG lasers. Finally, because the Brillouin frequency shift ν_B is inversely proportional to the pump wavelength, i.e., $\nu_B = 2nV_A/\lambda_p$, where n is the refractive index of silica, V_A is the acoustic velocity in silica, and λ_p is the pump wavelength, low noise microwave generation up to 32 GHz (as compared to 22 GHz using a 1550 nm pump [14]) is demonstrated using cascaded Brillouin laser lines at 1064 nm.

The experimental schematic is given in Fig. 1. A tunable continuous fiber laser is amplified by a Ytterbium-doped fiber amplifier (YDFA). In order to reduce the intensity noise induced by the YDFA, a RIN reduction setup comprised of an acousto-optical modulator (AOM), photodetector, and servo control is used. The intensity-stabilized pump laser is coupled to the disk resonator by a taper fiber [15,16]. The disk size ($D \approx 4$ mm) is designed such that its FSR matches the Brillouin shift frequency at 1064 nm ($\nu_B \sim 15.9$ GHz). As part of this design process, a frequency-modulation method was used for FSR measurement [17]. Larger disks ($D \approx 8$ and 16 mm) with FSR matching half and one-fourth of ν_B also were fabricated. A Pound–Drever–Hall (PDH) lock scheme—consisting of a phase modulator (PM), signal generator, mixer, and servo feedback—is used to lock the pump laser to the cavity resonance [18]. The SBS laser signal propagates opposite to the direction of the pump wave and is characterized using a photodetector and an optical spectrum analyzer. For laser frequency noise measurements, a Mach–Zehnder interferometer (MZI) also is used as an optical frequency discriminator (not shown in the figure). Finally, measured threshold pump power was in the range of 1 mW for loaded cavity linewidths ranging from 2 to 5 MHz.

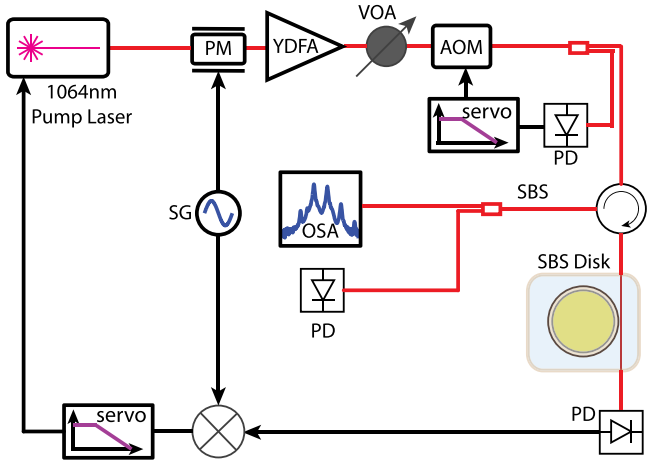

Fig. 1. Experimental schematic for characterization of 1064 nm SBS laser. Shown in the setup are PM, phase modulator; YDFA, Ytterbium-doped fiber amplifer; VOA, variable optical attenuator; AOM, acousto optic modulator; PD, photodetector; SG, signal generator; OSA, optical spectrum analyzer.

The frequency noise spectral density of the 1064 nm SBS laser was measured by a MZI with a FSR of 7.6 MHz. The laser was held at the quadrature point of the MZI in order to convert frequency noise to amplitude noise [12,19]. The inset of Fig. 2(a) shows the frequency fluctuation spectra measured for an 8 mm diameter device at a series of power levels. Above a few 100 kHz, the noise spectrum is approximately white, suggesting that this portion of the spectrum is associated with fundamental Schawlow–Townes noise. The two-sided, fundamental Schawlow–Townes frequency noise of the SBS laser can be written as [13]

$$S_\nu^{\mathrm{ST}}(f) = \frac{\hbar\omega^3}{8\pi^2 P Q_T Q_E}(n_T + N_T + 1), \tag{1}$$

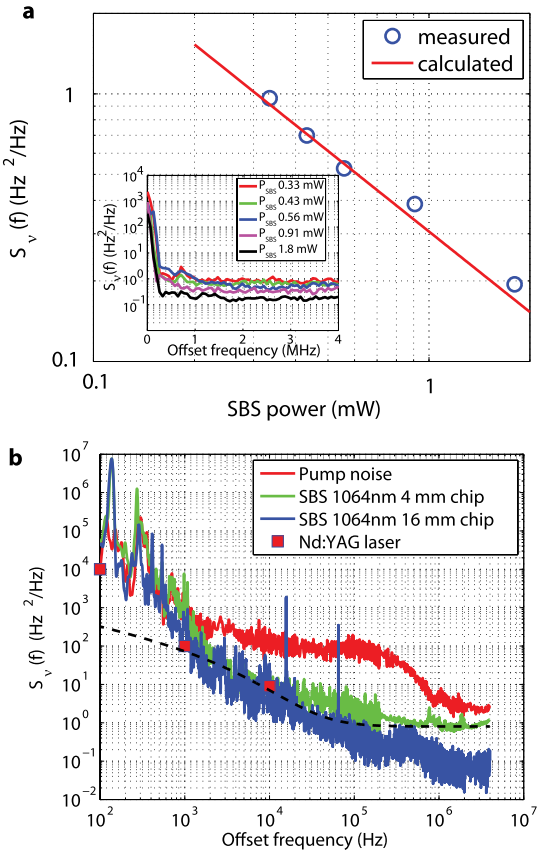

Fig. 2. (a) Inset: Frequency noise spectra for the SBS laser at 1064 nm measured at a series of laser output powers. The spectra are Schawlow–Townes noise limited for offset frequencies greater than a few 100 kHz. The device uses an 8 mm diameter cavity. Main panel: Schawlow–Townes noise level from the inset plotted versus output power and compared with the theoretically predicted Schawlow–Townes noise level. (b) Frequency noise spectra measured at offset frequencies less than 4 MHz for the pump laser (fiber laser, red curve), SBS laser from a 4 mm disk (green curve) and SBS laser from a 16 mm disk (blue curve). The Schawlow–Townes limit at high offset frequency is lower for the 16 mm device, as this device featured a higher optical Q factor. The red square markers are the frequency noise data for a narrow linewidth Nd:YAG laser (see text for reference). The black dashed line shows the calculated thermorefractive noise for a 4 mm microresonator plus a white Schawlow–Townes noise.

where $Q_{T,E}$ are the total and external Q factors, P is the output power of the Brillouin laser, and $n_T(N_T)$ is the number of thermal quanta in the mechanical (optical) field. N_T is negligible for optical frequencies, while $n_T \approx 386$ for a phonon frequency of 15.9 GHz at room temperature. The white noise level is plotted versus laser power in the main panel of Fig. 2(a). A theoretical curve based on the Schawlow–Townes formula agrees very well with the data.

The technical frequency noise of the 1064 nm SBS laser also was characterized and is shown in Fig. 2(b). The red curve is the frequency noise of the pump laser, while the green and blue curves give the frequency noise of SBS lasers based on 4 and 16 mm disks, respectively. The pump laser is a narrow linewidth Ytterbium-doped fiber laser, with an effective linewidth of 1 kHz. Its frequency-noise spectrum features a broad shoulder from 1 to 100 kHz. Significantly, the SBS laser frequency noise is suppressed relative to the pump laser for frequencies above 1 kHz. The technical noise between 1 and 50 kHz is close to the measured thermorefractive noise of the disk resonators [20]. Indeed, the measured decrease of the noise spectrum for the 16 versus the 4 mm disk is consistent with an expected decrease of thermorefractive noise with an increase of mode volume [20,21]. For comparison, the black dashed curve shows the calculated frequency-noise spectrum based on adapting a model of thermorefractive noise in a spherical resonator [21] to a 4 mm disk in a manner similar to that described in [22]. This thermorefractive noise component is added to a white Schawlow–Townes noise in the plot, i.e., $S_\nu(f) = S_\nu^{\mathrm{Thermo}}(f) + S_\nu^{\mathrm{ST}}(f)$. For even lower frequencies between 100 Hz and 1 kHz, the SBS laser frequency noise is believed to be limited by environmental mechanical and acoustic noise. For comparison, the red square markers give the frequency noise of a narrow-linewidth commercial Nd:YAG laser (Mephisto Laser, Coherent Inc., online data sheet [23]).

In addition to frequency noise, we also characterized the RIN of the on-chip SBS laser. Figure 3 shows the SBS laser RIN spectrum measured with the RIN reduction for the pump laser on and off. The servo control bandwidth for the RIN reduction was around 100 kHz. When the RIN reduction is off, the SBS laser RIN tracks the RIN shape of the pump laser + YDFA. The low-frequency behavior in this spectrum (1–100 kHz), as well as the noise spike at 65 kHz, is associated with the YDFA, while the noise bump between 100 kHz and 10 MHz is the fiber-laser relaxation oscillation resonance. The SBS laser RIN reaches a shot-noise-limited value of −141 dBc/Hz for frequencies greater than 20 MHz, when the incident optical power to the photodetector is 41 μW. When the RIN reduction is on, the pump laser intensity noise is stabilized below the locking bandwidth at 100 kHz, leading to the reduction of the SBS RIN within 100 kHz by a factor up to 20 dB. The low-frequency RIN of the SBS laser with the RIN reduction on is on the order of −125 dBc/Hz. Further reduction of the SBS laser RIN is currently under investigation.

Finally, low-noise microwave generation up to 32 GHz based on cascaded SBS lines in the 1064 nm band was demonstrated. When the intracavity power of the first Stokes line reaches the pump threshold for the

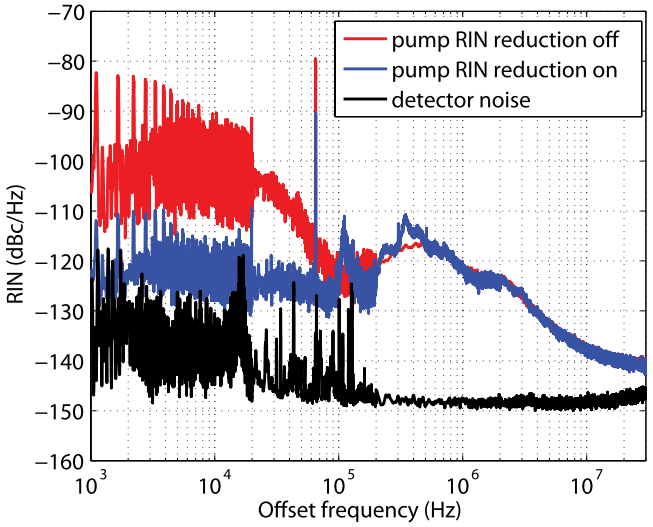

Fig. 3. RIN spectrum for the 1064 nm SBS laser with the pump laser RIN reduction "on" (blue curve) and "off" (red curve). Also shown is the detector noise (black curve).

second-order Stokes, the second Stokes line can start oscillation. Recently, we have demonstrated low-noise microwave synthesis up to 22 GHz (K band) based on heterodyne of the first and third Stokes lines in the 1550 nm band (where the Brillouin shift is around 10.8 GHz) [14]. The open- and closed-loop configuration for microwave generation based on the 1064 nm SBS lasers, shown in Fig. 4(a), is similar to that in the 1550 nm band [14]. However, a larger Brillouin shift at 1064 nm, i.e., $\nu_B \sim 1/\lambda_p$, leads to microwave generation with higher frequencies in the Ka band up to 32 GHz. In order to characterize the phase noise of the generated microwave signal, a phase-noise analyzer (PNA, Rohde Schwarz model number FSUP26) with a bandwidth up to 26.5 GHz is used. The beat note of 32 GHz measured directly from the fast photodetector with a bandwidth of 45 GHz is first divided to 4 GHz by an eightfold frequency divider and then measured by the PNA.

The center frequency of the microwave signal can be fine-tuned by varying the pump laser frequency. Thus it can be regarded as an optical voltage controlled oscillator (OVCO). The Fig. 4(b) inset shows the optical spectrum for the first and third Stokes lines measured in the back direction. Figure 4(b) shows the open-loop (free running OVCO) and closed-loop (phase lock-loop OVCO referenced to a low-frequency oscillator at 497 MHz) single-sideband phase noise of the 4 GHz signal. A phase noise level as low as −121 dBc/Hz at 100 kHz offset for the open loop case is achieved for the 4 GHz carrier.

In conclusion, we have demonstrated a narrow-linewidth SBS laser at 1064 nm from an on-chip ultra-high-Q silica wedge disk resonator. The fundamental Schawlow–Townes frequency noise of the SBS laser is on the order of 0.1 Hz^2/Hz. The technical frequency noise of the SBS laesr is close to the thermodynamic limit (thermorefractive noise) of the resonator at room temperature, with performance comparable to an ultra-narrow-linewidth Nd:YAG laser. The RIN of the SBS laser is suppressed by intensity stabilization of the pump laser. Finally, low-noise microwave synthesis up to 32 GHz using cascaded SBS lines is demonstrated.

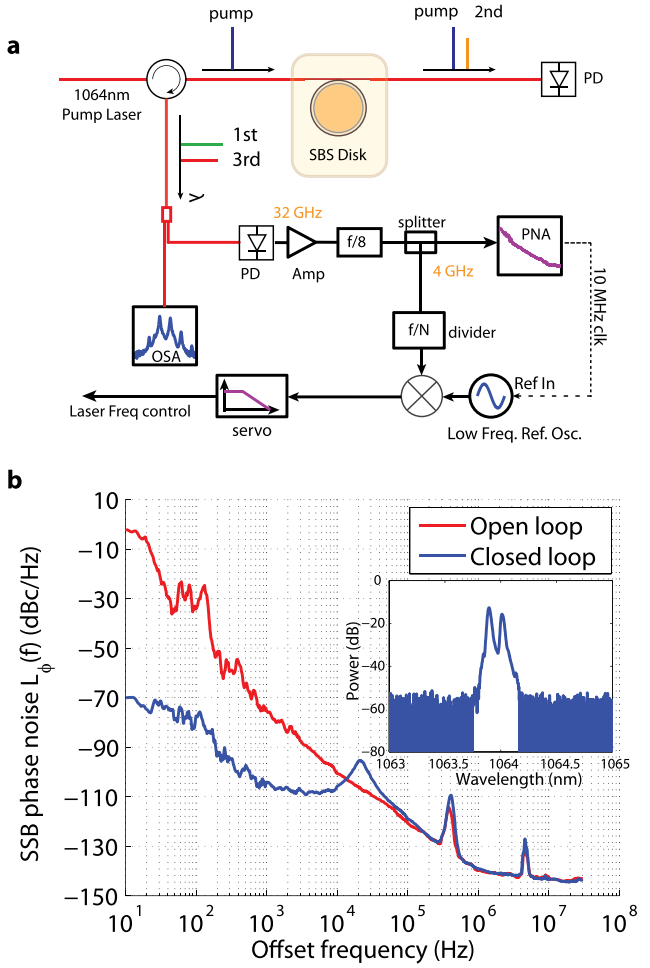

Fig. 4. (a) Schematic for microwave generation using the first and third SBS Stokes lines at 1064 nm. (b) Main panel: Single-sideband phase noise for the generated microwave at 4 GHz under open loop (free running) and closed loop (phase-lock loop with reference to a low-frequency reference oscillator at 497 MHz) cases. Inset: Optical spectrum of the first and third Stokes lines in the backward propagating direction.

We are grateful for financial support from the DARPA ORCHID and QUASAR programs, the Institute for Quantum Information and Matter (IQIM), the NSF Physics Frontiers Center with support of the Gordon and Betty Moore Foundation, and the Kavli NanoScience Institute.

References

1. R. J. Rafac, B. C. Young, J. A. Beall, W. M. Itano, D. J. Wineland, and J. C. Bergquist, Phys. Rev. Lett. **85**, 2462 (2000).
2. S. A. Diddams, Th. Udem, J. C. Bergquist, E. A. Curtis, R. E. Drullinger, L. Hollberg, W. M. Itano, W. D. Lee, C. W. Oates, K. R. Vogel, and D. J. Wineland, Science **293**, 825 (2001).
3. E. Ip, A. Lau, D. Barros, and J. Kahn, Opt. Express **16**, 753 (2008).
4. T. M. Fortier, M. S. Kirchner, F. Quinlan, J. Taylor, J. C. Bergquist, T. Rosenband, N. Lemke, A. Ludlow, Y. Jiang, C. W. Oates, and S. A. Diddams, Nat. Photonics **5**, 425 (2011).
5. C. Karlsson, F. Olsson, D. Letalick, and M. Harris, Appl. Opt. **39**, 3716 (2000).

6. A. Debut, S. Randoux, and J. Zemmouri, Phys. Rev. A **62**, 023803 (2000).
7. I. Grudinin, A. Matsko, and L. Maleki, Phys. Rev. Lett. **102**, 043902 (2009).
8. S. P. Smith, F. Zarinetchi, and S. Ezekiel, Opt. Lett. **16**, 393 (1991).
9. J. Geng, S. Staines, Z. Wang, J. Zong, M. Blake, and S. Jiang, IEEE Photon. Technol. Lett. **18**, 1813 (2006).
10. M. Tomes and T. Carmon, Phys. Rev. Lett. **102**, 113601 (2009).
11. R. Pant, C. G. Poulton, D. Choi, H. Mcfarlane, S. Hile, E. Li, L. Thevenaz, B. Luther-Davies, S. J. Madden, and B. J. Eggleton, Opt. Express **19**, 8285 (2011).
12. H. Lee, T. Chen, J. Li, K. Yang, S. Jeon, O. Painter, and K. J. Vahala, Nat. Photonics **6**, 369 (2012).
13. J. Li, H. Lee, T. Chen, and K. J. Vahala, Opt. Express **20**, 20170 (2012).
14. J. Li, H. Lee, and K. J. Vahala, Nat. Commun. **4**, 2097 (2013).
15. M. Cai, O. Painter, and K. J. Vahala, Phys. Rev. Lett. **85**, 74 (2000).
16. S. M. Spillane, T. J. Kippenberg, O. J. Painter, and K. J. Vahala, Phys. Rev. Lett. **91**, 043902 (2003).
17. J. Li, H. Lee, K. Y. Yang, and K. J. Vahala, Opt. Express **20**, 26337 (2012).
18. R. W. P. Drever, J. L. Hall, F. V. Kowalski, J. Hough, G. M. Ford, A. J. Munley, and H. Ward, Appl. Phys. B **31**, 97 (1983).
19. K. J. Williams, A. Dandridge, A. D. Kersey, J. F. Weller, A. M. Yurek, and A. B. Tveten, Electron. Lett. **25**, 774 (1989).
20. H. Lee, M. G. Suh, T. Chen, J. Li, S. A. Diddams, and K. J. Vahala, Nat. Commun. **4**, 2468 (2013).
21. M. L. Gorodetsky and I. Grudinin, J. Opt. Soc. Am. B **21**, 697 (2004).
22. A. Schliesser, G. Anetsberger, R. Riviere, O. Arcizet, and T. J. Kippenberg, New J. Phys. **10**, 095015 (2008).
23. For example, "Mephisto/Mephisto S Ultra-Narrow Linewidth CW DPSS Laser," https://www.coherent.com/downloads/Mephisto_CoherentDatasheet_Jan2013.pdf.